FULL PAPER DOI: 10.1002/adsc.202001549

Advanced Synthesis & Catalysis

Glycosyltransferase Co-Immobilization for Natural Product Glycosylation: Cascade Biosynthesis of the *C*-Glucoside Nothofagin with Efficient Reuse of Enzymes

Hui Liu,[a] Gregor Tegl,[a] and Bernd Nidetzky[a, b,*]

[a] Institute of Biotechnology and Biochemical Engineering, Graz University of Technology, NAWI Graz, Petersgasse 12, 8010 Graz, Austria
[b] Austrian Centre of Industrial Biotechnology (acib), Petersgasse 14, 8010 Graz, Austria
Fax: (+43)-316-873-8434
Phone: (+43)-316-873-8400
E-mail: bernd.nidetzky@tugraz.at

Manuscript received: December 10, 2020; Revised manuscript received: February 9, 2021;
Version of record online: March 2, 2021

Supporting information for this article is available on the WWW under https://doi.org/10.1002/adsc.202001549

Abstract: Sugar nucleotide-dependent (Leloir) glycosyltransferases are synthetically important for oligosaccharides and small molecule glycosides. Their practical use involves one-pot cascade reactions to regenerate the sugar nucleotide substrate. Glycosyltransferase co-immobilization is vital to advance multi-enzyme glycosylation systems on solid support. Here, we show glycosyltransferase chimeras with the cationic binding module Z_{basic2} for efficient and well-controllable two-enzyme co-immobilization on anionic (ReliSorb SP400) carrier material. We use the *C*-glycosyltransferase from rice (*Oryza sativa*; *Os*CGT) and the sucrose synthase from soybean (*Glycine max*; *Gm*SuSy) to synthesize nothofagin, the natural 3'-*C*-β-D-glucoside of the dihydrochalcone phloretin, with regeneration of uridine 5'-diphosphate (UDP) glucose from sucrose and UDP. Exploiting enzyme surface tethering via Z_{basic2}, we achieve programmable loading of the glycosyltransferases (~18 mg/g carrier; 60%–70% yield; ~80% effectiveness) in an activity ratio (*Os*CGT:*Gm*SuSy = ~1.2) optimal for the overall reaction rate (~0.2 mmol h^{-1} g^{-1} catalyst; 30 °C, pH 7.5). Using phloretin solubilized at 120 mM as inclusion complex with 2-hydroxypropyl-β-cyclodextrin, we demonstrate complete substrate conversion into nothofagin (~52 g/L; 21.8 mg product h^{-1} g^{-1} catalyst) at 4% mass loading of the catalyst. The UDP-glucose was recycled 240 times. The solid catalyst showed excellent reusability, retaining ~40% of initial activity after 15 cycles of phloretin conversion (60 mM) with a catalyst turnover number of ~273 g nothofagin/g protein used. Our study presents important progress towards applied bio-catalysis with immobilized glycosyltransferase cascades.

Keywords: Leloir glycosyltransferase; sugar nucleotide regeneration; co-immobilization; cascade bio-catalysis; *C*-glycosylation; nothofagin

Introduction

Sugar nucleotide-dependent (Leloir) glycosyltransferases are generally regarded as efficient and practically useful catalysts of glycosylation reactions.[1] In carbohydrate chemistry, glycosylation often represents the key central step of synthetic routes towards oligosaccharides,[1b,2] natural product glycosides[3] and glycoconjugates, including glycoproteins.[4] These are important product classes with promising applications in different commercial sectors, including medical healthcare in particular. The

use of glycosyltransferases in applied bio-catalysis must involve an integrated concept of reaction development.[1a] Like other enzymatic reactions that require (co)-substrates (e.g., nicotinamide coenzymes for oxidoreductions;[5] nucleoside triphosphates for phosphorylation[6] or nucleotide transfer;[7] *S*- adenosylmethionine for methylation[8]) which for reasons of atom economy and costs cannot be used stoichiometrically, the overall glycosyltransferase reaction typically consists of a multistep cascade transformation in which the immediate enzymatic glycosylation is supplied *in situ* with the corresponding sugar nucleotide donor substrate.[1,9] Besides synthesis from free monosaccharide via phosphorylation and nucleotide transfer cascades,[9a] sugar nucleotides are often prepared through a second glycosyltransferase reaction, run in reverse direction and operated in parallel to the synthetic reaction.[1a,3,9b] A suitably activated glycoside serves as the donor for *in situ* sugar nucleotide synthesis. A synthetically important example is the supply of uridine 5'-diphosphate (UDP) glucose (UDP-glucose) from sucrose and UDP, catalyzed by sucrose synthase (SuSy).[9b,10] Scheme 1 shows the glycosyltransferase cascade reaction of this study, involving the 3'-*C*-β-D-glycosylation of the dihydrochalcone phloretin from UDP-glucose that is continuously supplied and regenerated from UDP and sucrose. Nothofagin production according to Scheme 1 was used in our earlier studies[11] to demonstrate a systematic approach to process intensification for a glycosyltransferase cascade reaction, performed in batch conversion and in homogeneous solution. The current inquiry was set out to implement the same glycosyltransferase process on the surface of a solid support, with the aim of fundamental improvement in reaction efficiency due to a recyclable catalyst. Thus, the practical use of glycosyltransferases in glycoside synthesis could become substantially more operative. There has been high interest recently in the identification, characterization and engineering of Leloir *C*-glycosyltransferases[1a,3d,12] as well as in the use of these enzymes as catalysts of synthetically important *C*-glycosylation reaction.[13] The idea of this study, to develop a generic process technology for the application of immobilized glycosyltransferase cascades, is thus strongly supported. Advances made in the (semi) continuous synthesis of nothofagin, according to Scheme 1 and using co-immobilized enzymes, would seem to be largely transferrable to other *C*-glycosyltransferase-catalyzed glycosylation reactions from UDP-glucose of synthetic importance.[1a,13]

Immobilization is an important method from the general applied bio-catalysis toolbox for reaction development at the interface with process engineering.[14] Besides occasional reports scattered across glycosyltransferase types (e.g., sialyltransferase,[15a] galactosyltransferase,[15b] antibiotic glycosyltransferase,[15c] sucrose synthase[15d,e]), enzyme immobilization for (semi)continuous synthesis with reuse of solid catalyst is not well developed for the Leloir glycosyltransferases. In particular, broadly applicable technology for glycosyltransferase co-immobilization to establish glycosylation cascades on an insoluble support is lacking. Generally, co-immobilization (the colocalizing immobilization of multiple enzymes on the same solid carrier) can benefit the efficiency of heterogeneously catalyzed enzymatic cascade reactions by exploiting the effects of spatial proximity.[14c,16] Glycosyltransferase co-immobilization can be achieved in principle via immobilizing each enzyme according

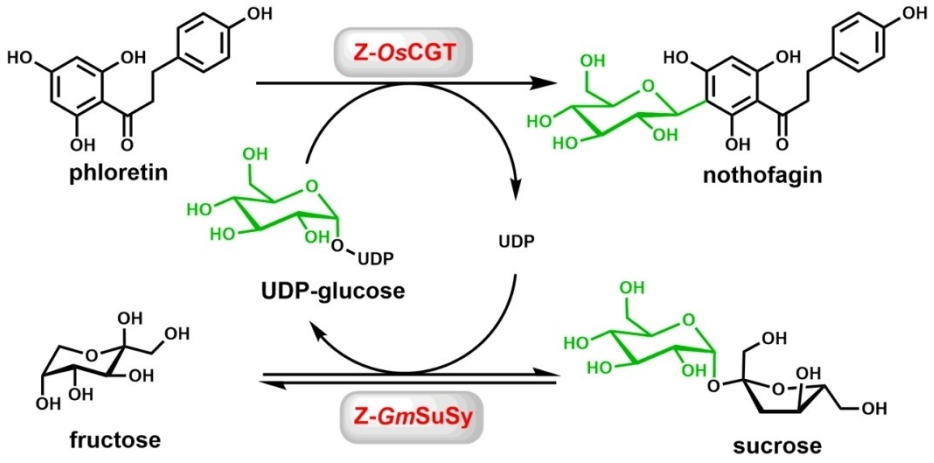

Scheme 1. Coupled glycosyltransferase reaction for nothofagin synthesis via 3'-*C*-β-glycosylation of phloretin from UDP-glucose which in turn is prepared from sucrose and UDP. The Z_{basic2} fusions of the rice (*Oryza sativa*) *C*-glycosyltransferase (*Os*CGT) and the soybean (*Glycine max*) sucrose synthase (*Gm*SuSy) are used as co-immobilized enzyme preparation on ReliSorb SP400. Catalytic amounts of UDP are used.

to its own, enzyme-specific strategy. Guisan, Rocha-Martin and coworkers have recently presented an important example of such "individualized" glycosyltransferase co-immobilization, applied to a natural product glycosyltransferase and a sucrose synthase, as discussed later in context of the evidence from the current study.[17] Alternatively, glycosyltransferase co-immobilization can be uniform in the strategy used for tethering the enzymes to the solid carrier surface. It is this latter strategy, realized in the form of glycosyltransferase fusions with the cationic binding module Z_{basic2}, that we have pursued here with the idea of a facile and efficient enzyme co-immobilization usable for nothofagin synthesis.

Z_{basic2} is a small protein of 58 amino acids and ~7 kilodalton size.[18] It is an engineered binding module, originally developed from the Z-domain of staphylococcal protein A. Placed within fusion proteins, the Z_{basic2} module can fold autonomously to adopt its stable three α-helical bundle structure.[18] Driven by electrostatic interactions from multiple arginine residues exposed on one of its sides,[18] the functional Z_{basic2} will bind with considerable affinity to negatively charged surfaces, such as those of cation exchange resins[19a] and silica materials.[19b] We have demonstrated fusion to Z_{basic2} for enzyme immobilization,[19] and recently also for multiple enzyme co-immobilization,[20] with excellent control, and modularity. Important elements of control are enzyme orientation on the solid surface, especially for co-immobilization, and relative amount of enzyme loaded onto the solid carrier. Moreover, enzymes immobilized via Z_{basic2} are homogeneously distributed in porous carriers,[19a,e] which is important to enable the co-localization of multiple enzymes. Cello-oligosaccharide synthesis from sucrose and glucose by three glycoside phosphorylases shows practical use of Z_{basic2}-based enzyme co-immobilization applied to a heterogeneously catalyzed cascade transformation.[19a]

Here, we present an efficient and flexible strategy for the co-immobilization of the rice (*Oryza sativa*) *C*-glycosyltransferase (*Os*CGT) and the soybean (*Glycine max*) sucrose synthase (*Gm*SuSy). Building on surface tethering via the Z_{basic2} module, this strategy is novel to the class of Leloir glycosyltransferases; and it opens up new important opportunities for development of a glycosyltransferase-based process technology for glycoside synthesis. Fusion to the Z_{basic2} module was reasonably tolerated as regards the enzyme specific activity (≥40% of the native glycosyltransferase). Single-enzyme immobilization as well as two-enzyme co-immobilization were demonstrated on ReliSorb SP400 carrier in good yield, 50–100% depending on the enzyme loading. The immobilized enzymes showed high catalytic effectiveness (≥50%). Programmable loading of the two glycosyltransferases gave an activity ratio (*Os*CGT:*Gm*SuSy = ~1.2) optimal for conversion of phloretin and sucrose into nothofagin. The solid catalyst was easily reusable, retaining ~40% of initial activity after 15 cycles of phloretin conversion (60 mM) with a catalyst turnover number of ~273 g nothofagin/g protein used. Our study presents important progress towards applied bio-catalysis with immobilized glycosyltransferase cascades.

Results and Discussion

Glycosyltransferase Fusions with Z_{basic2}

N-terminal fusions of *Os*CGT and *Gm*SuSy with the Z_{basic2} module were constructed and the resulting chimeric proteins obtained by expression in *E. coli*. The purified enzymes showed the expected mass for the respective full-length protein fused to Z_{basic2} (Figure S1). The specific activity of Z-*Os*CGT (2.06 U/mg) and Z-*Gm*SuSy (0.77 U/mg) was decreased to, respectively, 67% and 37% of the corresponding N-terminally Strep-tagged enzyme. Comparison of specific activities in purified enzyme and in cell lysate (Table S1) suggested that expression of Z_{basic2} protein was to a level of ~20–30% of total intracellular protein.

The Z-glycosyltransferases were conveniently recovered from the cell lysate (Figure S1). Moreover, as shown later, the Z-glycosyltransferases could be immobilized directly from cell lysate, without requirement for further enrichment and purification of the enzymes. The specific activity of *Os*CGT and *Gm*SuSy was decreased by ~40–60% in the presence of 250 mM NaCl. The effect was distinct for the Z-fusions of the glycosyltransferases. The Strep-tagged enzymes, by contrast, were unaffected by 250 mM NaCl (Table S1). The addition of 250 mM NaCl was considered because earlier studies of Z-enzyme immobilization[19] have shown that this can enhance the selectivity of the interaction of the Z_{basic2} module with the used ReliSorb SP400 carrier.

Single Enzyme Immobilization

The Z-glycosyltransferases were immobilized individually on ReliSorb SP400 resin (Figure S2 and Table S2). ReliSorb SP400 are polymethacrylate particles of spherical shape (75–200 μm diameter; 120 μm mean diameter) and involving a network of macro-pores with a size of ~100 nm. The ReliSorb SP400 material offers sulfonate surface groups as negatively charged interaction sites for oriented binding of the fusion protein via the cationic Z_{basic2} module.

Previous studies have shown excellent combination of efficiency and selectivity of Z-enzyme immobilization on ReliSorb SP400,[19a,20] encouraging our efforts here to directly immobilize the Z-glycosyltransferases from the cell lysate. Results in Figure S2 show

selective adsorption of both Z-*Os*CGT and Z-*Gm*SuSy to the ReliSorb SP400 carrier, leading to near-complete depletion of the target protein from cell lysate. Although the immobilized Z-glycosyltransferases were tethered non-covalently, their binding appeared to be strong: washing the carrier (~60 mg) two times with 1 mL of 50 mM HEPES buffer (pH 7.5; 250 mM NaCl) did not cause elution of enzyme activity.

As shown in Figure 1, we analyzed the individual immobilization of Z-*Os*CGT and Z-*Gm*SuSy on ReliSorb SP400 by monitoring, at different loadings of enzyme activity on the unit mass of carrier, the activity yield (% of the offered activity bound to the carrier) and the catalytic effectiveness (% activity retention) of the immobilized enzyme. The catalytic effectiveness is the ratio (×100, %) between the observable activity of the immobilized enzyme (U/g) and the activity expected for the immobilized enzyme based on the activity yield. For each enzyme, the observable activity increased dependent on the activity loaded, enabling an approximate range of 8–15 U/g for the active solid catalyst. The yield and the catalytic effectiveness both decreased with increasing enzyme loading, from a near 100% at the lowest loading to around 50–60% at the highest loading. The catalytic effectiveness of ~100% implies that no activity was lost as result of the Z-enzyme attachment to the solid carrier. The finding is as expected for a perfectly oriented immobilization of the Z-glycosyltransferase where the chimeric enzyme is tethered solely by its Z_{basic2} module and the function of the "catalytic module" is unaffected by the solid surface (for general discussion, see reference 14c). The decrease in catalytic effectiveness at higher enzyme loading might arise due to effects of enzyme crowding or aggregation on the solid surface. Pore clogging by immobilized enzyme might be another reason. It seems unlikely that at the enzyme loading used, the carrier was internally saturated with protein.[19a] In terms of protein immobilized, up to ~30 mg/g and ~42 mg/g were bound for Z-*Os*CGT and Z-*Gm*SuSy, respectively. Differences in protein binding may be due to the oligomer structure of the enzymes which differs for Z-*Os*CGT (monomer[11a]) and Z-*Gm*SuSy (homo-tetramer[10a]). Immobilization of Z-*Gm*SuSy might thus benefit from multivalent binding via two or more of its Z_{basic2} modules. Results of co-immobilized enzyme reuse experiments to be reported later show, however, that the Z-*Gm*SuSy was bound on the carrier not much more strongly than the monomeric Z-*Os*CGT. The structure of *Arabidopsis thaliana* SuSy[21] shows that the N-termini of neighboring protein subunits point to opposite sides of the enzyme tetramer. Structural constraints would therefore seem to limit the degree of multivalent binding in *Gm*SuSy immobilization to maximally two Z_{basic2} modules being involved simultaneously in tethering the enzyme tetramer to the solid surface. We presume at this stage, therefore, that multivalency effects in Z-*Gm*SuSy immobilization were small. The relatively similar behavior of the two Z-glycosyltransferases in terms of catalytic effectiveness, and dependence thereof on enzyme loading, is worth noting.

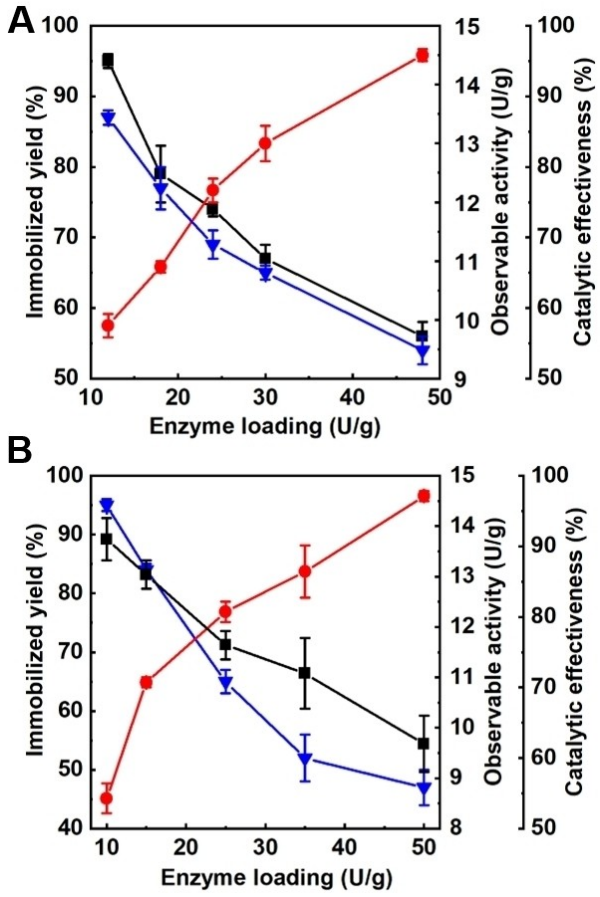

Figure 1. Immobilization of (A) Z-*Os*CGT and (B) Z-*Gm*SuSy on ReliSorb SP400. Enzymes were immobilized directly from the *E. coli* cell lysates. A 50 mM HEPES buffer (pH 7.5; 250 mM NaCl) was used for enzyme loading and washing. The carrier loading was 60 mg/ml. The buffer pH was unchanged during incubation. Immobilized yield (squares, black), observable activity (circles, red) and catalytic effectiveness (triangles, blue) are shown. Activities of soluble and immobilized enzymes were determined as described in the Methods.

Glycosyltransferase Co-Immobilization

Recent study suggests that immobilization of *O*-glycosyltransferase (from apple) and sucrose synthase (from *Acidithiobacillus caldus*) to co-localize the two enzyme activities on the same porous carrier benefits the synthetic efficiency of the bi-enzymatic glycosylation cascade.[17] The rate of 5-O-β-glycosylation of piceid (3-O-β-D-glucoside of resveratrol) was enhanced ~2.4-fold compared to reaction of the two enzymes immobilized individually on separate

carriers.[17] Therefore, to perform the 3-*C*-β-glycosylation of phloretin efficiently, we considered co-immobilization of *Os*CGT and *Gm*SuSy to place the enzymes closely together under the confinement of the solid surface. This would set particle radius of the carrier as the upper limit for the maximum diffusional distance in the reaction. Proximity effects could thus be exploited to maximize the overall flux through the two-step cascade reaction on solid support (for general discussion, see reference 16). We immobilized Z-*Os*CGT and Z-*Gm*SuSy in an activity ratio for the enzyme loaded that varied between 10.8 and 0.1. The maximum activity loaded was 43.2 U/g for Z-*Os*CGT (activity ratio 10.8) and 36 U/g for Z-*Gm*SuSy (activity ratio 0.1). For each activity ratio used, we measured the observable activity (rate of nothofagin synthesis) of the solid catalyst and the product yield from the coupled reaction. Figure 2A shows that both parameters passed through a maximum at an activity ratio of 1.2 and dropped sharply at lower and higher activity ratios. The optimum synthesis rate was ~13 U/g. Analysis with SDS PAGE (Figure 2B) reveals, for each activity ratio used, the protein distribution for Z-*Os*CGT and Z-*Gm*SuSy on the solid carrier. The semiquantitative picture from the polyacrylamide gel (Figure 2B) suggests that the activity ratio as loaded was largely retained in the solid catalyst. Using the optimum ratio of 1.2, we determined the observable activity for the individual enzymes (Z-*Os*CGT: 10.9 U/g; Z-*Gm*SuSy: 10.4 U/g) in the co-immobilized preparation. The Z-*Os*CGT and the Z-*Gm*SuSy were immobilized in a yield of ~60–70% and show an effectiveness of ~80%, both in good accordance with the results of single enzyme immobilization studies. These findings suggest that in Z-enzyme co-immobilization, the immobilization of one enzyme did not affect negatively the immobilization of the other. Generally, this is important as it enables programmable enzyme co-immobilization based on evidence from single enzyme immobilization experiments.

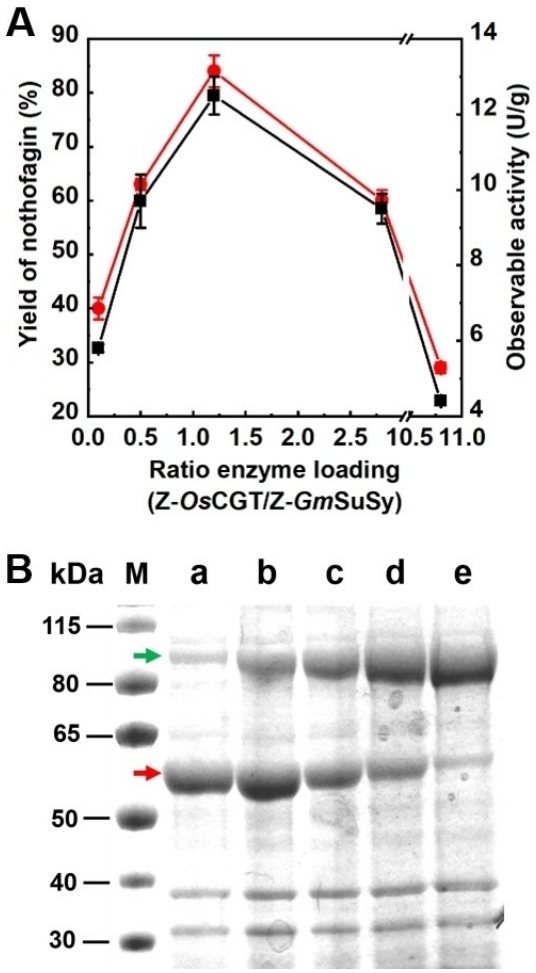

Figure 2. Co-immobilization of Z-*Os*CGT and Z-*Gm*SuSy on ReliSorb SP400. (A) Observable activity of nothofagin synthesis (squares, black) and nothofagin yield from the coupled reaction (circles, red) dependent on the activity ratio of Z-*Os*CGT and Z-*Gm*SuSy loaded. The co-immobilization was from *E. coli* lysates mixed in 50 mM HEPES buffer (pH 7.5; 250 mM NaCl). The activity measurements used the following conditions in 50 mM HEPES buffer (pH 7.5): 1 mM phloretin, 500 mM sucrose, 0.5 mM UDP, 13 mM $MgCl_2$, 50 mM KCl, 20% (by volume) DMSO, 1.3 mg/ml BSA; 30 °C and 1000 rpm agitation rate. (B) SDS polyacrylamide gel showing the proteins bound on ReliSorb SP400 dependent on the activity ratios loaded. The protein band corresponding to Z-*Os*CGT (red arrow) and Z-*Gm*SuSy (green arrow) is indicated. The activity ratio (Z-*Os*CGT/Z-*Gm*SuSy) was 10.8 (a), 2.8 (b), 1.2 (c), 0.5 (d), and 0.1 (e).

Characterization of the Co-Immobilized Glycosyltransferases

The pH dependence of activity for soluble and immobilized enzyme preparations was determined at 30 °C. As shown in Figure 3A, the activity of the soluble Z-*Os*CGT dropped sharply at high pH whereas the immobilized enzyme retained its maximum activity of pH 7.5 up to pH 10.5. For Z-*Gm*SuSy, the pH dependence of activity was relatively narrow, with optimum activity at pH of 6.5. Loss of activity at high pH was less pronounced in the immobilized enzyme (Figure 3B). Interestingly, an opposite trend was found at low pH where immobilized Z-*Gm*SuSy lost activity more dramatically than the soluble enzyme. In the co-immobilized enzyme preparation (Figure 3C), loss of activity at high pH was attenuated compared to the soluble enzymes. Considering the behavior of the single enzyme immobilized preparations (Figure 3A,B), the decrease in activity at high pH for the co-immobilized preparation appears to be dominated by the pH dependence of the Z-*Gm*SuSy activity. The optimum pH for the co-immobilized enzyme preparation was ~7.5.

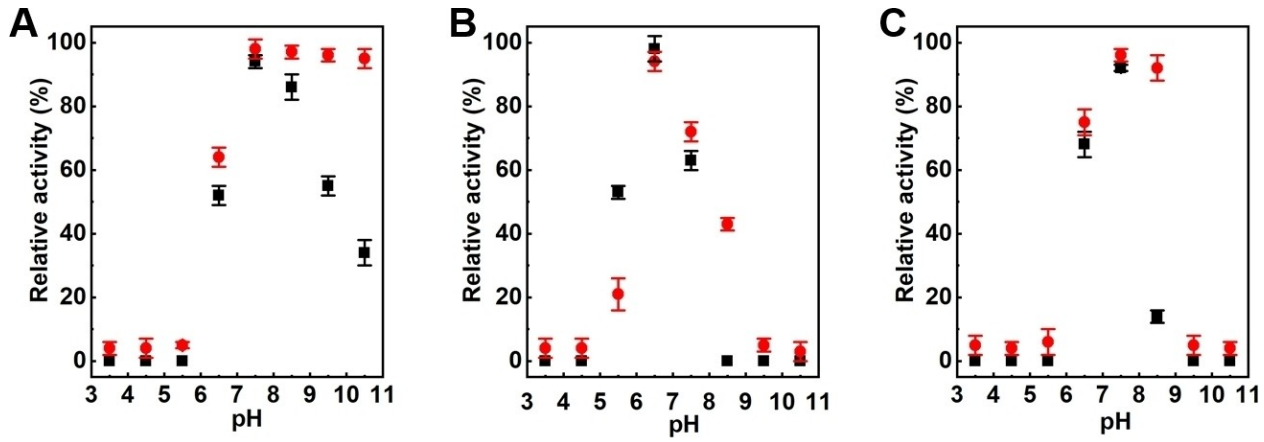

Figure 3. Effect of pH on the activity of the soluble (full squares, black) and the (co)-immobilized enzyme preparations (full circles, red). (A) Z-*Os*CGT, (B) Z-*Gm*SuSy, and (C) both enzymes used together in cascade reaction. The reaction buffers used were 25 mM sodium citrate/phosphate (pH 3.5–6.5), 50 mM HEPES (pH 7.5–8.5), and 50 mM CHES (pH 9.5.–10.5). The pH shown is the final pH of the suspension containing the carrier particles. Enzyme activities were measured as described in the Methods. The observable activity at the optimum pH (100%) was 14 U/g for immobilized Z-*Os*CGT, 13.5 U/g for immobilized Z-*Gm*SuSy and 13 U/g for the co-immobilized enzymes.

The temperature dependence of enzyme stability (30 min incubation) was analyzed at pH 7.5 by comparing soluble and immobilized enzyme preparations similarly as done for the pH-activity profiles. Results in Figure 4 (% activity loss dependent on temperature) reveal that except for Z-*Gm*SuSy that was more stable at 50 °C due to immobilization, the soluble and (co)-immobilized enzymes exhibited comparable stabilities. The idea of oriented immobilization via the Z_{basic2} module is that the characteristics of the enzyme module are largely unaffected by tethering of the Z-enzyme to the solid surface. One would, therefore, not expect a large stabilization of the activity of the Z-enzyme as result of the immobilization. An operational temperature range between 30 °C and 40 °C for the bi-enzymatic synthesis of nothofagin was suggested from the data in Figure 4.

Synthetic Activity and Recyclability of the Co-Immobilized Glycosyltransferases

The co-immobilized enzyme preparation (activity ratio 1.2) was used to examine its synthetic applicability and recyclability. Initially, to provide a proof of concept, a relatively low concentration of the phloretin substrate (1 mM) was used. The time course of nothofagin

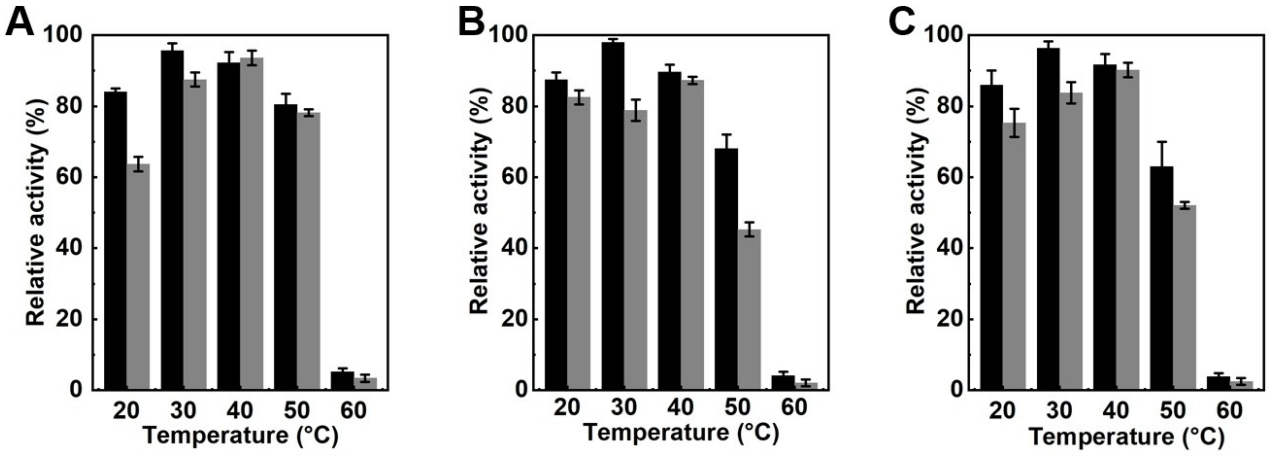

Figure 4. Thermostability of soluble (dark gray) and immobilized enzyme preparations (black). (A) Z-*Os*CGT, (B) Z-*Gm*SuSy, and (C) both enzymes used together in cascade reaction. Enzyme activities were measured as described in the Methods. Enzyme activities were measured as described in the Methods. The observable activity at the optimum pH (100%) was 14 U/g for immobilized Z-*Os*CGT, 13.5 U/g for immobilized Z-*Gm*SuSy and 13 U/g for the co-immobilized enzymes.

production is shown in Figure 5. The used phloretin was converted fully within ~15 min. The solid catalyst was recovered and the reaction was repeated 15 times. Figure 5B shows the nothofagin yield in each reaction of 15 min. The yield decreased gradually to ~60% in the last reaction. The solid catalyst was analyzed by SDS PAGE at reaction start and after the last reaction (Figure 5A). Comparison of the two samples reveals clear decrease in protein band intensity for both enzymes after repeated use of the catalyst. Despite the semiquantitative nature of the image, the loss in band intensity (Figure 5A), indicating partial elution of the non-covalently bound enzyme, might well account for the observed decrease in synthetic activity (Figure 5C).

Nothofagin Synthesis with Re-Use of the Co-Immobilized Glycosyltransferases

Due to the excellent recyclability of the co-immobilized enzyme preparation, we were encouraged to explore strategies of reaction intensification applicable to the solid catalyst. In particular, phloretin solubility should be enhanced to increase the product output. Using 20% DMSO co-solvent, the phloretin can be dissolved to ~10 mM and we show its full conversion from 5 mM or 10 mM initial concentration in Figure S3. To further increase the soluble phloretin concentration, we used inclusion complexation with 2-hydroxypropyl-β-cyclodextrin, as used by us previously for nothofagin production with the soluble enzymes.[11c] We show in Figure 6A that phloretin solubilized at 60 mM was converted very efficiently (≥98%) within ~12 h. The conversion rate (~0.2 mM/min) was even higher than in reactions using the non-complexed phloretin (~0.1 mM/min; Figure 5B, Figure S3). A space-time yield of ~5 mM/h (2.2 $g L^{-1} h^{-1}$) was calculated for the reaction run to completion. We increased the phloretin concentration to 120 mM and show its full conversion into nothofagin (Figure 6B). The time required for production was longer (60 h), due to a decreased initial conversion rate (~0.1 mM/min) and a pronounced slowing down of the reaction already at low degrees of conversion (~50%). The space-time yield of ~2 mM/h (0.87 $g L^{-1} h^{-1}$) was also decreased compared to the 60 mM reaction. Fluid viscosity which is increased strongly at high concentration of the phloretin inclusion complex with 2-hydroxypropyl-β-cyclodextrin[11c] could be a relevant factor. In a comparison at equivalent volumetric activity of the enzymes used, the solid catalyst was only about half as efficient in terms of space-time yield as the soluble enzymes. Viscosity effects are likely to be stronger in the heterogeneously catalyzed reaction and thus provide a possible explanation.

To examine re-use of the solid catalyst, we performed a total of 15 consecutive reactions with 60 mM phloretin, whereby each reaction lasted 12 h and involved recovery of the immobilized enzyme for the next reaction. As shown in Figure 7, the nothofagin yield decreased from a near 100% in the first reaction to ~40% in the last reaction. As in the re-use experiment in Figure 5, partial elution of enzyme from the solid catalysts (data not shown) seemed to be responsible for the gradual loss of catalyst efficiency over the number of reactions performed. We can calculate from the total nothofagin produced in the 15 reactions

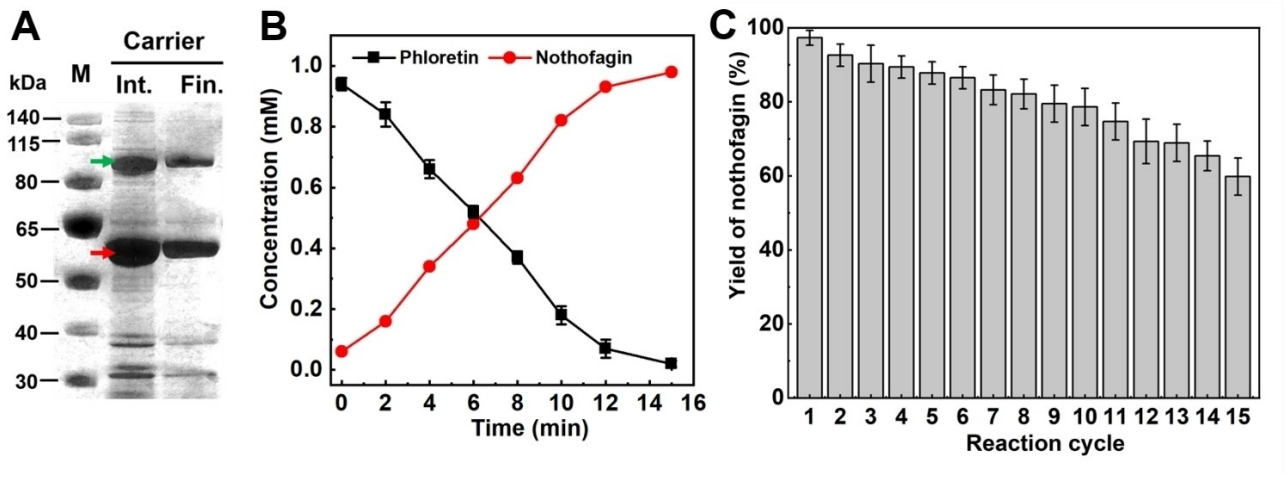

Figure 5. Synthetic activity and recyclability of co-immobilized Z-*Os*CGT and Z-*Gm*SuSy. (A) SDS polyacrylamide gel showing the protein on the ReliSorb SP400 carrier at reaction start (Int) and after the last reaction (Fin). (B) Reaction time course. (C) Repeated reaction as in panel B with reuse of the solid catalyst. Each reaction lasted 15 min. Conditions: 1 mM phloretin, 500 mM sucrose, 0.5 mM UDP, 50 mM KCl, 13 mM $MgCl_2$, 1.3 mg/ml BSA, 20% DMSO, 30 °C, 50 mM HEPES buffer (pH 7.5). The starting activity of immobilized Z-*Os*CGT and Z-*Gm*SuSy was 0.23 U/ml and 0.21 U/ml, respectively. The solid catalyst was used at 20 mg/ml. The loaded activity ratio was 1.2.

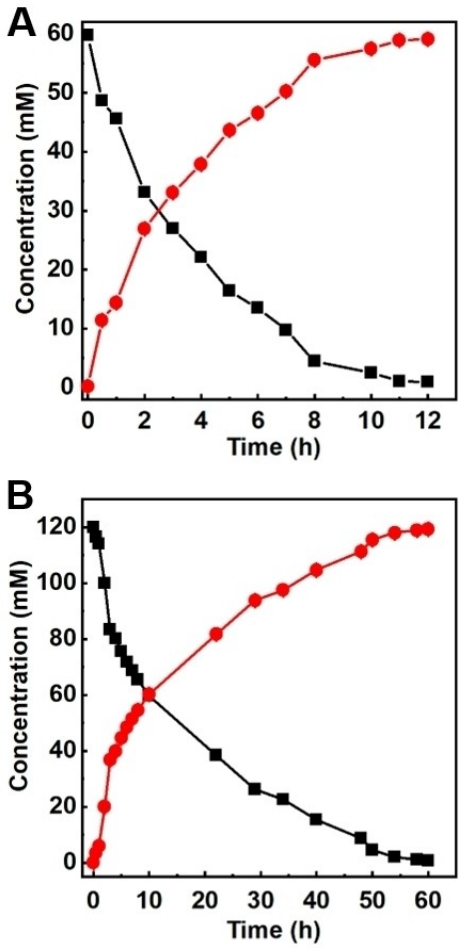

Figure 6. Nothofagin production (circles, red) from phloretin (squares, black) solubilized as inclusion complex with 2-hydroxypropyl-β-cyclodextrin (A, 60 mM; B, 120 mM) using co-immobilized Z-*Os*CGT and Z-*Gm*SuSy. Reaction conditions: 500 mM sucrose, 0.5 mM UDP, 50 mM KCl, 13 mM $MgCl_2$, 1.3 mg/ml BSA, 50 mM HEPES buffer (pH 7.5) and 30 °C. The starting activity of immobilized Z- *Os*CGT and Z-*Gm*SuSy was 0.47 U/ml and 0.42 U/ml, respectively. The solid catalyst was used at 40 mg/ml. The loaded activity ratio was 1.2.

(278 mg, 15 ml) and the amount of immobilized Z-*Os*CGT present on the solid catalyst (0.30 mg, recycled) that the *C*-glycosyltransferase reached a mass-based turnover number of 927 (= 278/0.30) g/g. With a M_r of 436 for nothofagin and 57,800 for Z-*Os*CGT, the corresponding mol-based turnover number is 1.2×10^5 mol/mol. Considering the Z-*Gm*SuSy (0.72 mg, recycled) that is additionally required, the mass-based turnover number becomes 273 (=278/1.02). These are excellent turnover numbers for a Leloir glycosyltransferase[1a,11a] and highlight the efficiency of the synthetic reaction when the solid catalyst is reused. It may be noted that nothofagin recovery from an enzymatic reaction mixture comparable to the ones obtained in Figure 6 and Figure 7 was demonstrated at 100 g scale in an earlier study from this laboratory.[11c] The isolated yield was ≥65% and the purity was ≥95%. Considering the product downstream processing to have been established in prior research, we did not pursue isolation of nothofagin in the current study.

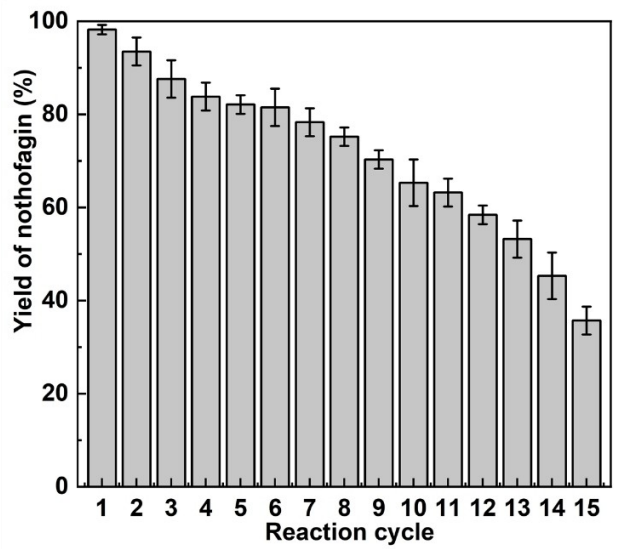

Figure 7. Re-use of the co-immobilized enzyme preparation for nothofagin production. Reaction conditions: 60 mM phloretin as inclusion complex with 2-hydroxypropyl-β-cyclodextrin, 500 mM sucrose, 0.5 mM UDP, 50 mM KCl, 13 mM $MgCl_2$, 1.3 mg/ml BSA, 50 mM HEPES buffer (pH 7.5) and 30 °C. The starting activity of immobilized Z-*Os*CGT and Z-*Gm*SuSy was 0.47 U/ml and 0.42 U/ml, respectively. The solid catalyst was used at 40 mg/ml. The loaded activity ratio was 1.2. Each reaction cycle lasted 12 h.

The Advantage of Enzyme Co-Immobilization for Efficient Glycosylation

Fusion to Z_{basic2} can introduce modular design to enzyme immobilization.[14c,19a,e] Unlike unstructured peptide tags, Z_{basic2} represents a structurally independent and functionally distinct unit (module) of the fusion protein. It can fold separately and provides a programmable function according to a uniform mechanistic principle of surface binding.[18] Due to its independent function in the modularly organized fusion protein, Z_{basic2} hardly interferes with the activity of its partner module, as shown for different enzymes previously[19,20,22] and here for the first time for representatives of the Leloir glycosyltransferase class. Thus, immobilization via Z_{basic2} is advantageous in particular when multiple enzymes in cascade biocatalysis should be tethered as a protein ensemble on a solid surface, to establish multistep reaction sequences on a single insoluble carrier. Proof of principle was shown from the co-immobilization of the Z-fusions of

three glycoside phosphorylases and the application of the solid catalyst thus obtained for cello-oligosaccharide synthesis.[20a] However, decision about enzyme co-immobilization on the same carrier, as opposed to single enzyme immobilization on different carriers, must balance gain in catalyst efficiency with increased complexity of catalyst preparation when co-immobilized enzymes are used.[16] We therefore set out experiments to compare co-immobilized preparation of Z-*Os*CGT and Z-*Gm*SuSy with a mixture of the individually immobilized enzymes for nothofagin synthesis under otherwise exactly comparable conditions. Time courses of conversion of 60 mM phloretin inclusion complex with 2-hydroxypropyl-β-cyclodextrin are shown in Figure 8. In both reactions, the phloretin was converted fully. In terms of initial reaction rate, reaction of the co-immobilized enzyme (34 mM/h) was ~2.5-fold faster than reaction of the individually immobilized enzymes. The space-time yield for full conversion (≥98%) was ~4-fold higher for the co-immobilized enzyme than for individually immobilized Z-*Os*CGT and Z-*Gm*SuSy. These results quantify the intensification of nothofagin production due to proximity effects of enzyme co-immobilization. The rate enhancement for the co-immobilized enzyme preparation can probably be ascribed to shortened diffusion paths when enzymes are co-localized on the porous surface of the solid carrier. Our results are consistent with study of Rocha-Martin and colleagues who showed 2.4-fold benefit of glycosyltransferase co-immobilization, compared to individual enzyme immobilization on separate carrier particles, on piceid glycosylation from sucrose-derived UDP-glucose.[17] The effect was dedicated to an enhanced efficiency of the UDP/UDP-glucose shuttle when enzymes are co-localized on the solid carrier.

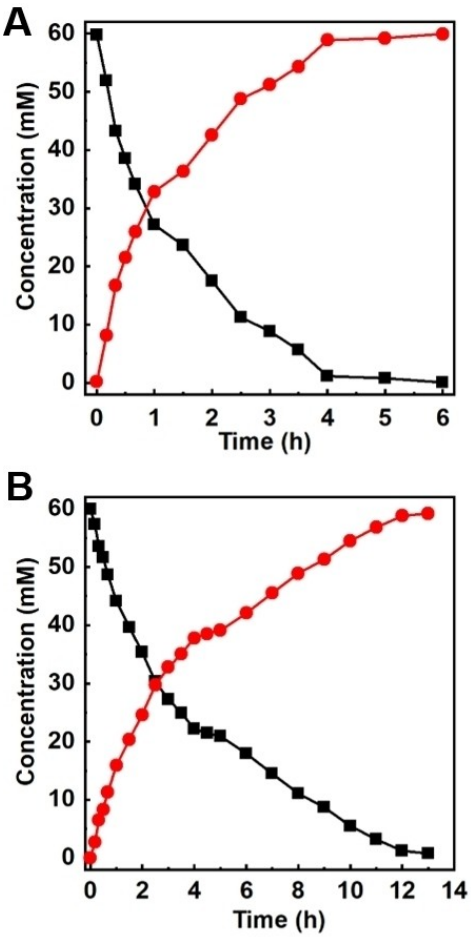

Figure 8. Synthesis of nothofagin using co-immobilized (A) or individually immobilized (B) enzyme preparations. Phloretin (squares, black) and nothofagin (circles, red) are shown. Reaction conditions: 60 mM phloretin as inclusion complex with 2-hydroxypropyl-β-cyclodextrin, 500 mM sucrose, 0.5 mM UDP, 50 mM KCl, 13 mM $MgCl_2$, 1.3 mg/ml BSA, 50 mM HEPES buffer (pH 7.5) and 30 °C. The starting activity of immobilized Z-*Os*CGT and Z-*Gm*SuSy was 1.17 U/ml and 1.05 U/ml, respectively. The solid catalyst was used at 100 mg/ml. The loaded activity ratio was 1.2.

Co-Immobilization of Z-*Os*CGT and Z-*Gm*SuSy in Context

Leloir glycosyltransferases are widely recognized for their synthetic importance.[1–4] They are considered "precision catalysts" of glycosylation with high potential for applied bio-catalysis. There have been limited efforts, however, to develop immobilized glycosyltransferases for heterogeneous catalysis applications (for reviews, see references 1a, 2a). Recently, Guisan, Rocha-Martin and their co-workers have shown immobilization of bacterial sucrose synthases on suitably activated agarose carriers.[15d] They also demonstrated glycosyltransferase co-immobilization on agarose,[17] as already discussed. Their studies showed glycosyltransferase immobilization in good loading (several mg protein/g carrier), high yield (≥50%) and typically good effectiveness (≥44%). Stabilization of tetrameric sucrose synthase required post-immobilization crosslinking.[15d] Re-use of the immobilized enzyme for up to 10 cycles was shown. Important advance made with the Z_{basic2} fusion approach reported here is fourfold. First, the immobilization no longer requires purified enzyme and is conveniently done from the cell lysate. Second, it builds on modular design. A proven engineering principle of enzyme tethering to the solid surface is flexibly applied to the (co)-immobilization of different glycosyltransferases. Efficiency parameters of the (co)-immobilization are good to excellent when applying standard immobilization conditions without enzyme-specific optimization. Third, a standard (anionic) carrier material can be used for immobilization without requirement for chemical derivatization/activation of the solid surface. Fourth,

enzyme co-localization on the solid carrier does not require specific adjustment and finely tuned control of the conditions for single-enzyme immobilization. Importantly, the co-immobilization study of Trobo-Maseda et al.[17] shows that unless proper control for enzyme co-localization is applied to the immobilization of the single enzymes, the effect of enzyme co-immobilization can be lost completely (~50-fold).

The lifetime of our co-immobilized glycosyltransferase catalyst is sufficient for multiple cycles of reaction. However, further stabilization of Z-enzyme binding to the solid surface will be important to enhance the turnover number of this catalyst. Post-immobilization techniques of protein crosslinking, as applied to sucrose synthase in the study of Trobo-Maseda et al.,[15d] may be useful. However, the enzyme turnover number from the current work (~273 g/g) shows Leloir glycosyltransferases to be already on par with other enzymes (e.g., glycoside hydrolases,[23] glycoside phosphorylases[20a,24] perceived as more robust for application in glycosylation.

Conclusion

Modular bioengineering is a powerful approach for accelerated development in biotechnology.[25] Fusion to the Z_{basic2} module is shown here for glycosyltransferase co-immobilization to implement sugar nucleotide-dependent glycosylation cascade reactions on solid support. The example of Z-*Os*CGT and Z-*Gm*SuSy demonstrates convenient production of the Z-glycosyltransferases in *E. coli* and programmable enzyme co-immobilization in a facile, high-yielding procedure directly from the cell lysates. The solid catalyst with Z-*Os*CGT and Z-*Gm*SuSy loaded in optimum ratio shows excellent overall activity for nothofagin synthesis from sucrose and phloretin, and it can be recycled conveniently from the reaction. Output parameters, such as yield, product concentration, space-time yield, and recycling of UDP as catalytic reagent, are similar for batch syntheses by soluble and co-immobilized enzymes. Recycling of the co-immobilized enzymes enhances the enzyme turnover number by another ≥10-fold. Collectively, this study emphasizes enzyme co-immobilization as an important element of a comprehensive process intensification strategy for glycosylation reactions catalyzed by coupled Leloir glycosyltransferases.

Experimental Section

Materials

ReliSorb SP400 carrier was from Resindion (Binasco, Italy). 2-Hydroxypropyl-β-cyclodextrin (>98%), phloretin (>98%), UDP (97%) and UDP-glucose (>98%) were from Carbosynth (Compton, UK). Other chemicals were of reagent grade. Further materials used are described in the Supporting Information. Authentic standard of nothofagin (phloretin 3'-*C*-β-D-glucoside; ≥99%) was obtained from recent study using enzymatic synthesis.[11c]

Z-Enzymes

*Os*CGT (GenBank id: FM179712) and *Gm*SuSy (GenBank id: AF030231) were used. Enzyme chimeras harboring the Z_{basic2} module fused to the N-terminus were constructed from the plasmid vector pT7_Z_P450 BM3[20c] using overlap extension PCR. The oligonucleotide primers used (Table S1) and the PCR conditions applied are found in the Supporting Information. The used expression vectors are referred to pT7_Z_*Os*CGT and pT7_Z_*Gm*SuSy. The relevant protein sequences and the methods used for protein expression in *E. coli* BL21(DE3) and purification by cation exchange chromatography are detailed in the Supporting Information. Protein purification was monitored by SDS PAGE and measurement of specific enzyme activity. Enzymes harboring N-terminal Strep-tag II have previously been reported[11a] and are used as reference. Protein concentrations were measured with ROTI Quant assay (Carl Roth, Karlsruhe, Germany) referenced against BSA. Z-*Os*CGT (~15 mg/ml) and Z-*Gm*SuSy (~20 mg/ml) were stored in 50 mM HEPES buffer (pH 7.5) at −20 °C. Enzyme preparations retained full activity for at least 2 weeks.

The cell lysates used for immobilization were prepared by ultrasonication of *E. coli* cells suspended in a 2-fold volume of 50 mM HEPES buffer (pH 7.5). A Sonic Dismembrator Model 505 (Fisher Scientific, Vienna, Austria) was used and the sonication protocol (6 min in total) involved alternating 3 s pulse on and 9 s pulse off at 60% amplitude and cooling on ice. Cell lysate was recovered by centrifugation (15,000 rpm, 4 °C, 40 min; Centrifuge 5424R, Eppendorf, Vienna, Austria).

Enzyme Assays

Reactions were performed in 1 ml total volume at 30 °C in 2 ml plastic tubes using agitation at 400 rpm (soluble enzymes) or 1000 rpm (immobilized enzymes) in an Eppendorf ThermoMixer C instrument (Vienna, Austria). Samples (20 µl) were withdrawn after 5, 10 and 20 min and reactions quenched with the same volume of acetonitrile. Solid material (precipitated protein, immobilization carrier) was centrifuged off (13200 rpm, 4 °C, 20 min; Centrifuge 5424R, Eppendorf) and the supernatant analyzed by ion-pairing reversed-phase HPLC.[26] A Shimadzu model UFLC HPLC system equipped with a Kinetex® 5 µm EVO C18 LC column (100 Å, 150×4.6 mm; Phenomenex, Merck, Vienna, Austria) was used. The column was equilibrated at 25 °C in 20 mM potassium phosphate buffer (pH 5.9) containing 40 mM tetrabutylammonium bromide. Elution was with acetonitrile. UV detection was used.

Z-*Os*CGT. The reaction mixture contained in 50 mM HEPES buffer (pH 7.5), 1 mM phloretin, 2 mM UDP-glucose, 13 mM $MgCl_2$, 50 mM KCl, 4% DMSO, and 1.3 mg/ml BSA. NaCl (250 mM) was added optionally. HPLC analysis used an acetonitrile gradient (20%–50%) at 1 ml/min and detection at 282 nm. Rates were determined from [nothofagin]/time. One

unit (U) of activity is the enzyme amount releasing 1 µmol nothofagin/min under the conditions used.

Z-*Gm*SuSy. The reaction mixture contained in 50 mM BisTris buffer (pH 6.5), 500 mM sucrose, 2 mM UDP, 13 mM $MgCl_2$, 50 mM KCl and 1.3 mg/ml BSA. NaCl (250 mM) was added optionally. HPLC analysis used isocratic acetonitrile conditions (12.5%) at 2 ml/min and detection at 262 nm. Rates were determined from [UDP-glucose]/time. One U is the enzyme amount releasing 1 µmol UDP-glucose/min under the conditions used.

Coupled reaction. The reaction mixture contained in 50 mM HEPES buffer (pH 7.5), 1 mM phloretin, 500 mM sucrose, 0.5 mM UDP, 13 mM $MgCl_2$, 50 mM KCl, 20% DMSO and 1.3 mg/ml BSA. HPLC analysis of the Z-*Os*CGT assay was used. Rates were determined from [nothofagin]/time. One U is the enzyme amount releasing 1 µmol nothofagin/min under the conditions used.

Immobilization

ReliSorb SP400 carrier (60 mg dry material) was weighed into 2 ml Eppendorf tubes, washed three times with water and afterwards two times with HEPES buffer (50 mM, 250 mM NaCl, pH 7.5). The pH of the carrier suspension was verified as 7.5. For single enzyme immobilization, *E. coli* cell lysate (1 ml; 2–15 mg total protein/ml) was added and incubated at room temperature at 40 rpm on an end-over-end rotator for 2 h. Supernatant was removed and carrier washed twice with 50 mM HEPES (pH 7.5; Z-*Os*CGT) or 50 mM Bistris (pH 6.5; Z-*Gm*SuSy) buffer, each containing 250 mM NaCl. Supernatant and washing solutions were collected for protein and activity measurements. The pH was always checked and was constant at ~7.5. The carrier was also recovered and used for activity measurement. For enzyme co-immobilization, *E. coli* cell lysates containing Z-*Os*CGT and Z-*Gm*SuSy were mixed in variable volume ratio (10.8–0.1) to give 1 ml of total lysate to be added to 60 mg dry carrier. The mixture was incubated (50 mM HEPES buffer, pH 7.5; 250 mM NaCl) and processed as described above. The individual activities of Z-*Os*CGT and Z-*Gm*SuSy as well as the combined (coupled) activity of the two enzymes were measured using the assays already stated. Unless mentioned, in the co-immobilization experiment activity refers to the coupled reaction.

Parameters used to evaluate the immobilization were the following.

Loaded activity. This is the enzyme activity loaded on the carrier and is expressed as U/g. Cell lysates used for immobilization had a known volumetric activity (U/ml) and protein concentration (mg/ml). The activity loaded was calculated from the protein loaded in the experiment.

Bound activity. This is the activity bound to the solid carrier. It was calculated as difference in the soluble enzyme activity (U) before (A_0) and after the immobilization (A). The activity A is the total activity present in the supernatant of the immobilization and the washing solutions. The bound activity is calculated as ΔA ($=A_0-A$) divided by the carrier mass (g). The bound activity is expressed as U/g.

Immobilization yield. This is expressed as $\Delta A/A_0$ (×100, %).

Observable activity. This is the activity of the solid catalyst directly measured in an activity assay. It is expressed as U/g.

Catalytic effectiveness. This is the ratio of observable

activity and bound activity (×100, %). Immobilizations were performed in triplicates and the mean value with standard error is reported.

Immobilized Enzyme Characterization

The pH-activity profile of soluble and (co)-immobilized enzymes was recorded at 30 °C in the pH range 3.5–10.5. The buffers used were 25 mM sodium citrate/phosphate (pH 3.5–6.5), 50 mM HEPES (pH 7.5–8.5), and 50 mM CHES (pH 9.5–10.5). The other reaction conditions and the analytical procedures used were the ones of the enzyme assays described above. The pH values given are from the suspension of carrier particles. Enzyme stability at different temperatures in 10 °C interval between 20 °C and 60 °C were recorded in 50 mM HEPES buffer (pH 7.5) and using incubation for 30 min. Residual activity was then recorded at 30 °C using the standard activity assays. In pH and temperature studies, purified preparations of the soluble enzymes were used. The soluble enzyme concentration used was typically ~0.1 mg/ml, equivalent to ~0.2 U/ml. The volumetric concentration of the immobilized enzyme, as prepared from loading cell lysate on ReliSorb SP400, was ~0.25 U/ml. The co-immobilized enzyme preparation involved a ~1.2 activity ratio of Z-*Os*CGT and Z-*Gm*SuSy loaded on the carrier.

Enzymatic Synthesis of Nothofagin

Formation of the phloretin inclusion complex. 2-Hydroxypropyl-β-cyclodextrin (4.2 g; 3 mmol) was dissolved to ~300 mM in ~4 ml of deionized water in a 50 ml tube. Microwave heating at 750 W was used. The total heating time was ~20 s and several steps of heating and mixing by inversion were used. Phloretin (0.66 g; 2.4 mmol; ~240 mM) was added and dissolved as before. Not all phloretin could be dissolved with the procedure used. The final volume was set to 10 ml. The mixture was equilibrated in a drying chamber at 70 °C for 1 h and inverted every 15 min. If required, the solution was stored overnight at 4 °C and microwave-heated shortly prior to use. Insoluble phloretin was centrifuged off (5000 rpm, 5 min, room temperature). In each conversion experiment, the actual phloretin concentration in solution was determined by HPLC.

Enzymatic conversion. Reactions were performed using non-complexed phloretin at low concentrations (1.0–10 mM; 20% DMSO cosolvent) or phloretin inclusion complex (60 mM, 120 mM; no cosolvent). For 1 mM phloretin (20% DMSO cosolvent), the reaction was performed in 50 mM HEPES buffer (pH 7.5) containing 20 mg/ml solid catalyst, 500 mM sucrose, 0.5 mM UDP, 50 mM KCl, 13 mM $MgCl_2$ and 1.3 mg/ml BSA. A total liquid volume of 500 µl was used. For 60 mM phloretin inclusion complex, the reaction was performed in 50 mM HEPES buffer (pH 7.5) containing 40 mg/ml solid catalyst, 500 mM sucrose, 0.5 mM UDP, 50 mM KCl, 13 mM $MgCl_2$ and 1.3 mg/ml BSA. A total liquid volume of 1 ml was used.

Unless mentioned, a 1.2 activity ratio of Z-*Os*CGT and Z-*Gm*SuSy loaded on the carrier was used. Especially note, the term of solid catalyst refers to the enzymes co-immobilized on Relisorb SP400 throughout the manuscript. The volumetric activities varied as indicated in the text. The temperature was 30 °C and agitation was at 1000 rpm in an Eppendorf ThermoMixer C. Samples (30 µl) were taken at certain times and processed as described above for the assay of the coupled reaction. All reactions were performed in triplicates and the mean value with standard error is reported.

Re-use of co-immobilized enzymes. At the end of the enzymatic reaction, the solid carrier was centrifuged off (4000 rpm, 20 min, 4 °C; Centrifuge 5424R, Eppendorf) and the supernatant withdrawn for analysis. The carrier washed twice with 50 mM HEPES buffer (pH 7.5) and then resuspended in 500 µl (1 mM) or 1 ml (60 mM) fresh reaction mixture for a consecutive round of conversion. Incubation was done for a set time (15 min, 12 h) depending on the phloretin concentration (1 mM, 60 mM) used. The carrier re-use was done 15 times.

Enzyme turnover determination. We define the turnover number as the mass nothofagin produced in 15 reaction cycles/mass enzyme used. To determine the total enzyme mass applied on solid carrier in the reaction, we used the observable activity of each Z-*Os*CGT and Z-*Gm*SuSy (U/g carrier) as the basis. The observable activity was corrected for the known catalytic effectiveness of the immobilized enzyme (Z-*Os*CGT: 77%; Z-*Gm*SuSy: 76%), yielding the bound activity of the immobilized enzyme if it were fully active. This activity was divided by the specific activity of the purified enzyme, thus giving the mg of each Z-*Os*CGT and Z-*Gm*SuSy used on carrier in the reaction. The mol-based turnover number was calculated with the M_r of nothofagin (436) and Z-*Os*CGT (57800).

Acknowledgements

Martin Pfeiffer, Peter Wied and Chao Zhong (Institute of Biotechnology and Biochemical Engineering, Graz University of Technology) are acknowledged for their support. H.L. is recipient of fellowship from the China Scholarship Council (grant number 201906380025).

References

[1] a) B. Nidetzky, A. Gutmann, C. Zhong, *ACS Catal.* **2018**, *8*, 6283–6300; b) L. Krasnova, C. H. Wong, *J. Am. Chem. Soc.* **2019**, *141*, 3735–3754; c) L. Mestrom, M. Przypis, D. Kowalczykiewicz, U. Hanefeld, P. L. Hagedoorn, *Int. J. Mol. Sci.* **2019**, *20*, 5263.

[2] a) S. Schelch, C. Zhong, B. Petschacher, B. Nidetzky, *Biotechnol. Adv.* **2020**, *44*, 107613; b) M. M. Nielsen, C. M. Pedersen, *Chem. Rev.* **2018**, *118*, 8285–8358; c) L. Wen, G. Edmunds, C. Gibbons, Y. Kong, P. G. Wang, *Chem. Rev.* **2018**, *118*, 8151–8187; d) H. Yu, X. Chen, *Org. Biomol. Chem.* **2016**, *14*, 2809–2818.

[3] a) R. W. Gantt, P. Peltier-Pain, J. S. Thorson, *Nat. Prod. Rep.* **2011**, *28*, 1811–1853; b) D. M. Liang, J. H. Liu, H. Wu, B. B. Wang, H. J. Zhu, J. J. Qiao, *Chem. Soc. Rev.* **2015**, *44*, 8350—8374; c) W. Schwab, T. C. Fischer, A. Giri, M. Wüst, *Appl. Microbiol. Biotechnol.* **2015**, *99*, 165–174; d) G. Tegl, B. Nidetzky, *Biochem. Soc. Trans.* **2020**, *48*, 1583–1598.

[4] a) C. Li, L. X. Wang, *Chem. Rev.* **2018**, *118*, 8359–8413; b) P. Bojarová, R. R. Rosencrantz, L. Elling, V. Křen, *Chem. Soc. Rev.* **2013**, *42*, 4774–4797.

[5] a) Y. Wang, H. Ren, H. Zhao, *Crit. Rev. Biochem. Mol.* **2018**, *53*, 115–129; b) J. J. Dong, E. Fernández-Fueyo, F. Hollmann, C. E. Paul, S. Younes, W. Zhang, *Angew. Chem. Int. Ed.* **2018**, *57*, 9238–9261; *Angew. Chem.* **2018**, *130*, 9380–9404; c) S. Wu, R. Snajdrova, J. C. Moore, K. Baldenius, U. T. Bornscheuer, *Angew. Chem. Int. Ed.* **2020**, *59*, 2–34; d) R. Yuryev, S. Strompen, A. Liese, *Beilstein J. Org. Chem.* **2011**, *7*, 1449–1467.

[6] a) S. Mordhorst, J. Singh, M. K. F. Mohr, R. Hinkelmann, H. J. Jessen, J. N. Andexer, *ChemBioChem* **2019**, *20*, 1019–1022; b) J. N. Andexer, M. Richter, *ChemBioChem* **2015**, *16*, 380–386.

[7] S. C. Timmons, R. H. Mosher, S. A. Knowles, D. L. Jakeman, *Org. Lett.* **2007**, *9*, 857–860.

[8] C. Liao, F. P. Seebeck, *Nat. Catal.* **2019**, *2*, 696–701.

[9] a) W. Li, J. B. McArthur, X. Chen, *Carbohydr. Res.* **2019**, *472*, 86–97; b) B. Sauerzapfe, L. Elling, In: *Multistep Enzyme Catalysis: Biotransformations and Chemoenzymatic Synthesis, 1st ed.*, Eds.: E. Garcia-Junceda, Wiley-VCH, Weinheim, **2008**, pp. 83–102.

[10] a) K. Schmölzer, A. Gutmann, M. Diricks, T. Desmet, B. Nidetzky, *Biotechnol. Adv.* **2016**, *34*, 88–111; b) A. Zervosen, L. Elling, In: *Carbohydrate Biotechnology Protocols: Methods in Biotechnology, 1st ed., Vol. 10*, Eds: C. Bucke, Springer, **1999**, pp. 235–254.

[11] a) L. Bungaruang, A. Gutmann, B. Nidetzky, *Adv. Synth. Catal.* **2013**, *355*, 2757–2763; b) L. Bungaruang, A. Gutmann, B. Nidetzky, *Adv. Synth. Catal.* **2016**, *358*,486–493; c) K. Schmölzer, M. Lemmerer, B. Nidetzky, *Biotechnol. Bioeng.* **2018**, *115*, 545–556.

[12] a) N. Putkaradze, D. Teze, F. Fredslund, D. H. Welner, *Nat. Prod. Rep.* **2021**, doi.org/10.1039/D0NP00040 J; b) J. B. He, P. Zhao, Z. M. Hu, S. Liu, X. Qiao, M. Ye, *Angew. Chem. Int. Ed.* **2019**, *58*, 11513–11520; c) M. Zhang, F. D. Li, K. Li, X. Qiao, M. Ye, *J. Am. Chem. Soc.* **2020**, *142*, 3506–3512; d) F. Mendoza, G. A. Jaña, *J. Chem. Inf. Model.* **2020**, *60*, 933–943; e) Z. L. Wang, H. M. Wang, S. Zhang, X. Qiao, M. Ye, *Proc. Mont. Acad. Sci.* **2020**, *117*, 30816–30823.

[13] a) D. Chen, R. Chen, R. Wang, X. Yu, J. Dai, *Angew. Chem. Int. Ed.* **2015**, *127*, 12869–12873; b) D. Chen, S. Fan, R. Chen, Z. Yang, J. Dai, *ACS Catal.* **2018**, *8*, 4917–4927; c) D. Chen, R. Chen, K. Xie, F. Ye, J. Dai, *Org. Lett.* **2018**, *20*, 1634–1637; d) K. Xie, X. Zhang, S. Sui, F. Ye, J. Dai, *Nat. Commun.* **2020**, *11*, 1–12.

[14] a) U. Hanefeld, L. Gardossi, E. Magner, *Chem. Soc. Rev.* **2009**, *38*, 453–468; b) R. C. Rodrigues, C. Ortiz, Á. Berenguer-Murcia, R. Torres, R. Fernández-Lafuente, *Chem. Soc. Rev.* **2013**, *42*, 6290–6307; c) J. Boudrant, J. M. Woodley, R. Fernandez-Lafuente, *Process Biochem.* **2020**, *90*, 66–80; d) C. Mateo, J. M. Palomo, G.

Fernandez-Lorente, J. M. Guisan, R. Fernandez-Lafuente, *Enzyme Microb. Technol.* **2007**, *40*, 1451–1463; e) J. M. Bolivar, B. Nidetzky, *Bioch. Biophys. Acta - Proteins Proteom.* **2020**, *1868*, 140333; f) J. M. Bolivar, I. Eisl, B. Nidetzky, *Catal. Today* **2016**, *259*, 66–80; g) C. Garcia-Galan, Á. Berenguer-Murcia, R. Fernandez-Lafuente, R. C. Rodrigues, *Adv. Synth. Catal.* **2011**, *353*, 2885–2904; h) O. Barbosa, C. Ortiz, Á. Berenguer-Murcia, R. Torres, R. C. Rodrigues, R. Fernandez-Lafuente, *Biotechnol. Adv.* **2015**, *33*, 435–456.

[15] a) H. Kajiwara, M. Tsunashima, T. Mine, Y. Takakura, T. Yamamoto, *J. Biosci. Bioeng.* **2016**, *121*, 390–393; b) R. Schneider, M. Hammel, E. G. Berger, O. Ghisalba, J. Nuesch, D. Gygax, *Glycoconjugate J.* **1990**, *7*, 589–600; c) Z. Chen, J. Zhang, S. Singh, P. Peltier-Pain, J. S. Thorson, B. J. Hinds, *ACS Nano.* **2014**, *8*, 8104–8112; d) L. Trobo-Maseda, A. H. Orrego, S. Moreno-Pérez, G. Fernández-Lorente, J. M. Guisan, J. Rocha-Martin, *Appl. Microbiol. Biotechnol.* **2018**, *102*, 773–787; e) A. H. Orrego, L. Trobo-Maseda, J. Rocha-Martin, J. M. Guisan, *Enzyme Microb. Technol.* **2017**, *105*, 51–58.

[16] S. Arana-Peña, D. Carballares, R. Morellon-Sterlling, R. C. Rodrigues, R. Fernandez-Lafuente, *Biotechnol. Adv.* **2020**, doi.org/10.1016/j.biotechadv.2020.107584.

[17] L. Trobo-Maseda, A. H. Orrego, J. M. Guisan, J. Rocha-Martin, *Int. J. Biol. Macromol.* **2020**, *157*, 510–521.

[18] a) T. Gräslund, M. Hedhammar, M. Uhlén, P. Å. Nygren, S. Hober, *J. Biotechnol.* **2002**, *96*, 93–102; b) M. Hedhammar, S. Hober, *J. Chromatogr. A* **2007**, *1161*, 22–28.

[19] a) J. Wiesbauer, J. M. Bolivar, M. Mueller, M. Schiller, B. Nidetzky, *ChemCatChem* **2011**, *3*, 1299–1303; b) J. M. Bolivar, B. Nidetzky, *Langmuir* **2012**, *28*, 10040–10049; c) J. M. Bolivar, B. Nidetzky, *Biotechnol. Bioeng.* **2012**, *109*, 1490–1498; d) J. M. Bolivar, S. Schelch, T. Mayr, B. Nidetzky, *ACS Catal.* **2015**, *5*, 5984–5993; e) D. Valikhani, J. M. Bolivar, M. Pfeiffer, B. Nidetzky, *ChemCatChem* **2017**, *9*, 161–166; f) J. M. Bolivar, C. Luley-Goedl, E. Leitner, T. Sawangwan, B. Nidetzky, *J. Biotechnol.* **2017**, *257*, 131–138.

[20] a) C. Zhong, B. Duić, J. M. Bolivar, B. Nidetzky, *ChemCatChem* **2020**, *12*, 1350–1358; b) M. B. Buergler, A. Dennig, B. Nidetzky, *Biotechnol. Bioeng.* **2020**, *117*, 2377–2388; c) D. Valikhani, J. M. Bolivar, A. Dennig, B. Nidetzky, *Biotechnol. Bioeng.* **2018**, *115*, 2416–2425.

[21] Y. Zheng, S. Anderson, Y. Zhang, R. M. Garavito, *J. Biol. Chem.* **2011**, *286*, 36108–36118.

[22] P. García-García, J. Rocha-Martin, J. M. Guisan, G. Fernandez-Lorente, *Catalysts* **2020**, *10*, 810.

[23] a) E. M. H. F. Bongers, J. M. Opitz, A. Fryer, P. Sarda, B. C. J. Hamel, N. V. A. M. Knoers, *Am. J. Med. Genet.* **2001**, *102*, 115–124; b) B. Zeuner, C. Jers, J. D. Mikkelsen, A. S. Meyer, *J. Agric. Food Chem.* **2014**, *62*, 9615–9631; c) K. Schmölzer, M. Weingarten, K. Baldenius, B. Nidetzky, *ACS Catal.* **2019**, *9*, 5503–5514; d) L. Ruzic, J. M. Bolivar, B. Nidetzky, *Biotechnol. Bioeng.* **2020**, *117*, 1597–1602; e) S. W. Jang, C. H. Cho, Y. S. Jung, H. S. Shin, D. H. Seo, *PLoS One* **2018**, *13*, e0207466; f) Y. Malbert, C. Moulis, I. André, M. Remaud-Simeon, *Sci. Rep.* **2018**, *8*, 15153; g) M. Benkoulouche, R. Fauré, M. Remaud-Siméon, C. Moulis, I. André, *Interface Focus* **2019**, *9*, 20180069; h) K. Slámová, J. Kapešová, K. Valentová, *Int. J. Mol. Sci.* **2018**, *19*, 1–19; i) I. Bassanini, J. Kapešová, L. Petrásková, H. Pelantová, K. Markošová, M. Rebroš, K. Valentová, M. Kotik, K. Káňová, P. Bojarová, J. Cvačka, L. Turková, E. E. Ferrandi, I. Bayout, S. Riva, V. Křen, *Adv. Synth. Catal.* **2019**, *361*, 2627–2637.

[24] a) T. Desmet, W. Soetaert, P. Bojarová, V. Křen, L. Dijkhuizen, V. Eastwick-Field, A. Schiller, *Chem. Eur. J.* **2012**, *18*, 10786–10801; b) J. Franceus, T. Desmet, *Int. J. Mol. Sci.* **2020**, *21*, 2526; c) K. De Winter, K. Verlinden, V. Křen, W. Soetaert, T. Desmet, *Green Chem.* **2013**, *15*, 1949–1955; d) K. De Winter, G. Dewitte, M. E. Dirks-Hofmeister, S. De Laet, H. Pelantová, V. Křen, T. Desmet, *J. Agric. Food Chem.* **2015**, *63*, 10131–10139; e) M. Kraus, C. Grimm, J. Seibel, *ChemBioChem* **2016**, *17*, 33–36; f) M. E. Dirks-Hofmeister, T. Verhaeghe, K. De Winter, T. Desmet, *Angew. Chem.* **2015**, *127*, 9421–9424; *Angew. Chem. Int. Ed.* **2015**, *54*, 9289–9292.

[25] a) S. Garcia, C. T. Trinh, *Biotechnol. Adv.* **2019**, *37*, 107403; b) C. T. Trinh, B. Mendoza, *Curr. Opin. Chem. Eng.* **2016**, *14*, 18–25; c) K. Yu, C. Liu, B. G. Kim, D. Y. Lee, *Biotechnol. Adv.* **2015**, *33*, 155–164; d) C. J. Hartley, C. C. Williams, J. A. Scoble, N. J. Turner, C. Scott, *Nat. Catal.* **2019**, *2*, 1006–1015.

[26] A. Gutmann, A. Lepak, M. Diricks, T. Desmet, B. Nidetzky, *Biotechnol. J.* **2017**, *12*, 1600557.